Bull. Mater. Sci. (2018) 41:37
https://doi.org/10.1007/s12034-018-1559-5

Controllable factors affecting the epitaxial quality of $LaCoO_3$ films grown by polymer-assisted deposition

YANPING ZHANG[1,2], HAIFENG LIU[2,*], RUISHI XIE[2], GUOHUA MA[2], JICHUAN HUO[2] and HAIBIN WANG[3]

[1]School of Materials Science and Engineering, Southwest University of Science and Technology, Mianyang 621010, People's Republic of China

[2]Analytical and Testing Center, Southwest University of Science and Technology, Mianyang 621010, People's Republic of China

[3]School of Chemistry and Chemical Engineering, Mianyang Normal University, Mianyang 621010, People's Republic of China

*Author for correspondence (haifengliu2010@hotmail.com)

MS received 24 April 2017; accepted 22 July 2017; published online 23 March 2018

Abstract. $LaCoO_3$ epitaxial films grown on (100) $SrTiO_3$ substrates were prepared by the simple polymer-assisted deposition successfully. Based on the characteristics by X-ray diffractometer, infrared spectroscopy and thermal analyzer, the influence of molecular weight of polyethyleneimine, heat-treatment condition, spin-coating speed on the crystallinity and epitaxial quality of $LaCoO_3$ films were discussed. It is found that the number of –NH groups plays a key role in the cation-chelation of polyethyleneimine. Comparatively, more –NH groups existing in polyethyleneimine with larger molecular weight contribute to the improvement of epitaxial quality of $LaCoO_3$ epitaxial film. When polyethyleneimine begins to release the bound metal ions, higher heat-treatment temperature and a relatively rapid rate of heating can effectively prevent nucleus from growing in other orientations, thereby improving the epitaxial quality of film. Besides, the choice of spin speed will directly affect the thickness and surface roughness of the film, and may even affect the structure and performance of the film. The results will help to understand the cation-chelation mechanism of polyethyleneimine in the polymer-assisted deposition and extend this simple method for preparation of epitaxial films.

Keywords. Polymer-assisted deposition; $LaCoO_3$; epitaxial film; polyethyleneimine.

1. Introduction

Polymer-assisted deposition (PAD) is a simple and cost-effective technique to prepare various metal-oxide epitaxial films comparing with traditional physical or chemical vapour depositions [1,2], radio-frequency sputtering [3], molecular beam epitaxy [4] and pulsed laser deposition (PLD) [5], which need complicated equipment and have the difficulty of making large-area films. Among the aqueous solution deposition techniques, sol–gel [6,7], metal-organic deposition [8], chemical solution deposition [9] and electrochemical deposition [10] were reported to prepare epitaxial films, but many metal oxides cannot be deposited and sometimes the stoichiometry and uniformity are out of control effortlessly owing to differences in chemical reactivity among the metals [11]. The PAD method is a new aqueous solution deposition technique for growth of epitaxial film. In comparison, it has overcome those shortcomings effectively. In this process, an aqueous solution of metal-precursors is mixed with a soluble polymer which actively binds, encapsulates the metal ions and helps to prevent both hydrolysis reactions and make them evenly distribute in solution, growing high-quality epitaxial films with desired chemical composition accordingly [12–17]. Therefore, it has motivated much recent research on the preparation and properties of simple or complex metal-oxides epitaxial films by PAD method, such as VO_2 [13], $PrNiO_3$ [14], $Ba_{1-x}Sr_xTiO_3$ [15] and Re_2NiMnO_6 [16]. However, there are almost no reports directly researching on the mechanism and controllable factors in this method. No doubt, further research is necessary for extending the application of PAD method.

Thus, in this work, we selected polyethyleneimine (PEI) as a soluble polymer and prepared $LaCoO_3$ (LCO) epitaxial films on (100)-oriented $SrTiO_3$ (STO) single-crystal substrates. Then, we analysed three factors influencing the quality of LCO epitaxial films grown on STO substrates by PAD method, namely, molecular weight of PEI, heat-treatment condition and spin-coating speed. Based on the characteristics for the crystal structure, thermal decomposition and chelate bonding, epitaxial nature of the LCO films and cation-chelation mechanism during the preparation were investigated.

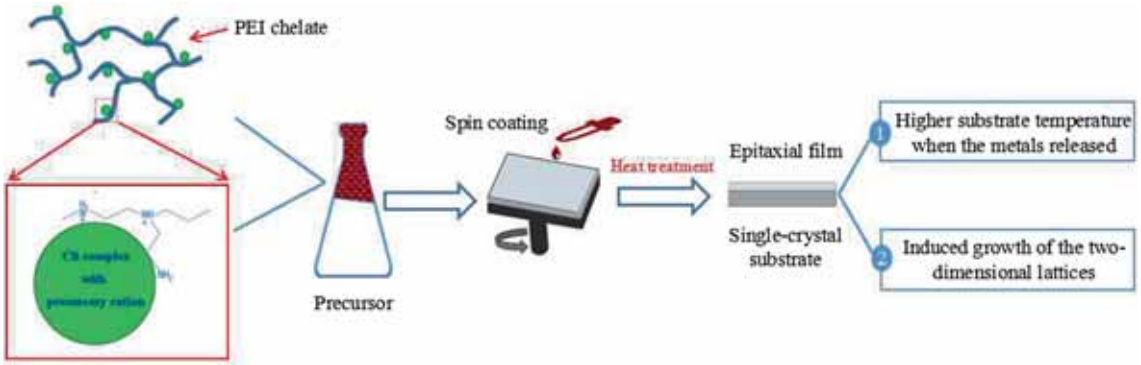

Figure 1. Schematic diagrams of the epitaxial growth mechanism of LCO films.

2. Experimental

2.1 *Thin film preparation*

The precursor solution of LCO was prepared as follows. First, metal salts $La(NO_3)_3 \cdot nH_2O$ (0.5 mmol) and $Co(NO_3)_2 \cdot 6H_2O$ (0.5 mmol) were mixed and dissolved in 5 ml deionized water. Then, ethylenediaminetetraacetic acid (EDTA) (1 mmol) was added. After 30 min chelating-reaction, high-purity (>99%) PEI (0.2922 g) with different molecular weights (M = 600, 1800, 10 k and 70 k) was dissolved in about 10 ml deionized water and dripped into the above solution slowly using a dropper. The mixed solution was stirred by a magnetic stirring apparatus for 12 h at room temperature, and then kept being stirred in a 60°C oil bath until ~5 ml solution remained. Consequently, the fuchsia precursor solution of reasonable viscosity was achieved.

Subsequently, the precursor solution was deposited on single-crystal (100)-oriented STO substrates (10 mm × 5 mm × 0.5 mm) at 2000, 4000, 5500 and 7000 rpm over 30 s by a spin-coating technique, respectively. Then, the coated substrates were placed in a muffle furnace and heated up at a certain heating rate from room temperature to a certain temperature. After 2 h heat treatment, the films were cooled down to room temperature at 1°C min^{-1}. Finally, the epitaxial films were obtained under different heat treatment conditions.

2.2 *Characterization*

The structural and epitaxial characterizations of the films including $\theta/2\,\theta$ symmetric scan and ω-scans (rocking curve) were performed via a X-ray diffractometer (XRD) with CuKα radiation (PANalytical X'Pert PRO, λ = 1.54187 Å). The bonding characteristics of product during the process of PEI chelating La^{3+} and Co^{2+} were investigated by an infrared spectroscopy (IR, US PE Company, Spectrum One) ranging from 400 to 4000 cm^{-1} at room temperature. In addition, the pyrolysis properties of the chelates were measured by a synchronous thermal analyzer (US TA Instrument Company, SDT Q600) from room temperature to 800°C. The thickness of the film was obtained by a field emission scanning electron microscope (FESEM, Carl Zeiss, Ultra 55).

3. Results and discussion

3.1 *Growth mechanism of LCO epitaxial film by PAD method*

Figure 1 shows the epitaxial growth mechanism of LCO films. The PAD process mainly includes the following steps. The first step is the preparation of precursor solution of LCO. Firstly, EDTA is used preliminarily to chelate La^{3+} and Co^{2+} ions, and form small molecule complexes. Since the aqueous solution of PEI is alkaline and the precipitation pH value of La^{3+} and Co^{2+} ions is about 7, La^{3+} and Co^{2+} ions may precipitate and cannot be bound to the polymer chain of PEI polymer if the PEI solution is directly added into the nitrate solution. Followed by the PEI chelating process, which is the key step of PAD method, the active groups of the PEI molecular chain bind the small chelate (i.e., the small molecule complex formed by the EDTA and La^{3+}, Co^{2+} ions) in the solution to the molecular chain, thereby forming a stable precursor solution. In this process, PEI has dual functions. On the one hand, as a binding agent to the metal precursor, PEI can effectively bind the metal ions to form a stable bonding effect and prevent hydrolysis reaction. On the other hand, the controlled solution concentration and the molecular weight of PEI can help to achieve the desired viscosity and to prepare a relatively thick and crack-free film. This dual effect of PEI may be different from its role in the preparation of quantum dots, in which PEI is mainly used to disperse quantum dots and prevent their reunion [18,19]. The second step is the spin-coating process. The above precursor solution with a certain viscosity is deposited on single-crystal substrates to form a thin film by the spin-coating method. The third step is the heat-treatment process. A low-heating rate from room temperature to 500°C is used to make sure the solvent evaporated and polymers burnt-up to avoid the formation of pinholes and cracks even polycrystalline film. The metal ions

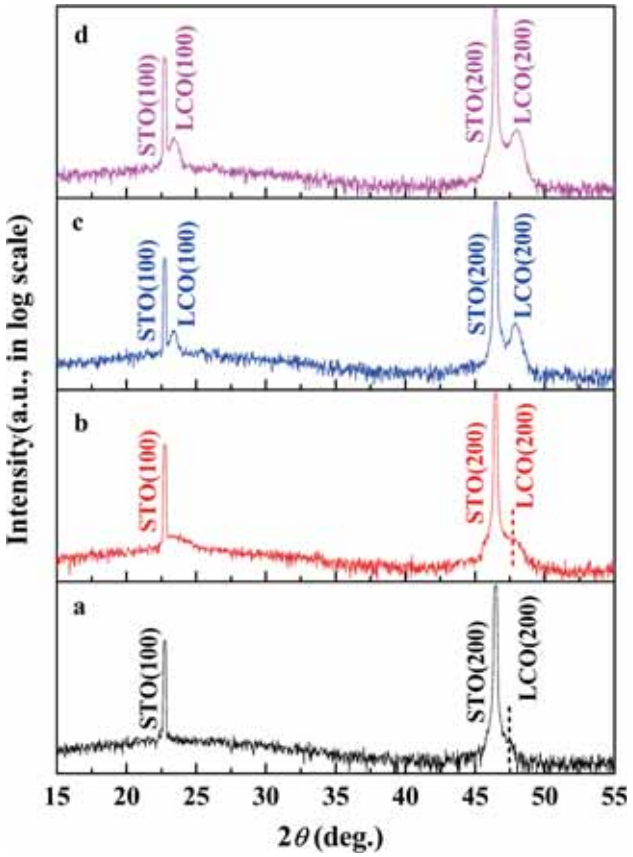

Figure 2. XRD patterns of $\theta/2\theta$ scans for the LCO films grown with PEI of different molecular weights: (**a**) 600, (**b**) 1800, (**c**) 10 k and (**d**) 70 k, respectively. PEI with larger molecular weight corresponds to better epitaxial quality.

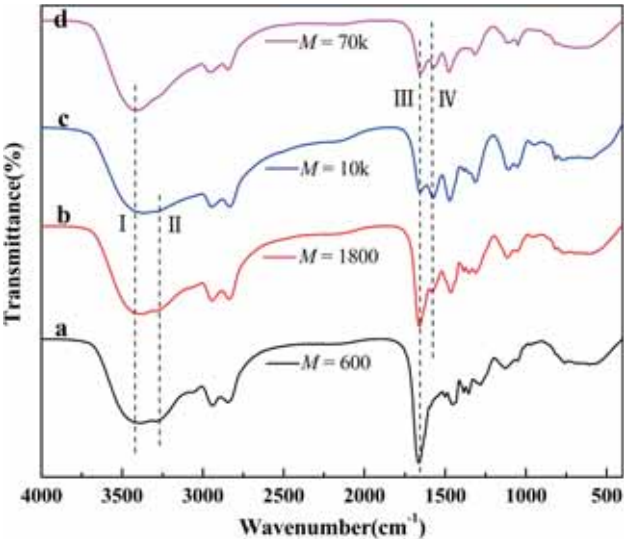

Figure 3. IR spectra of PEI with different molecular weights: (**a**) 600, (**b**) 1800, (**c**) 10 k and (**d**) 70 k, respectively. More –NH, but less $–NH_2$ exists in PEI with larger molecular weight. Peak I and II refer to N–H stretching vibration of –NH and $–NH_2$, respectively; peak III and IV refer to N–H bending vibration of $–NH_2$ and –NH, respectively.

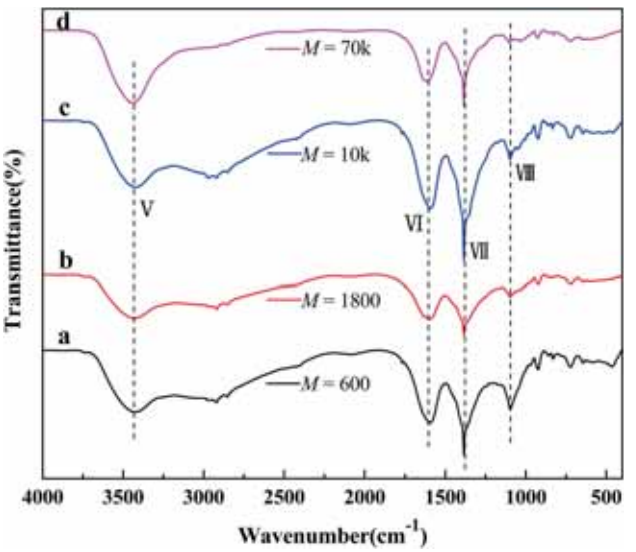

Figure 4. IR spectra of chelate grown with PEI of different molecular weights: (**a**) 600, (**b**) 1800, (**c**) 10 k and (**d**) 70 k, respectively. The number of –NH groups dominate the cation-chelation of PEI. Peak V, VI, VII and VIII refer to the vibration of O–H, coordinated –COO, C–H and C–O, respectively.

are released to form oxides after the decomposition of polymer (450−500°C), and the higher substrate temperature is conducive to the growth of epitaxial film [11]. Then, the film is rapidly heated to a relatively higher temperature to prevent the generation of massive nucleation and improve the epitaxy and crystallinity [15,20], thus, growing into an epitaxial film induced by the two-dimensional lattices of single-crystal substrate.

In the PAD process, the polymer acting as a trapping agent for metal ions plays a crucial role, which is the major difference between PAD and existing sol–gel or chemical solution deposition processes [21–24]. Besides, the PAD method has some advantages over other chemical solution deposition methods. Firstly, the precursor solution is more stable because the polymer confines the metal ions to prevent its hydrolysis. Secondly, the presence of polymer greatly reduces the shrinkage and the generation of partial stresses in the film during the phase formation, which makes it possible to grow relatively thicker and crack-free metal-oxide films. What's more, a relatively higher substrate temperature when the bound metals released is more favourable for the growth of epitaxial film [11,12].

3.2 *Effect of PEI molecular weight on the crystallinity and epitaxial quality of LCO films*

The typical XRD patterns for the LCO/(100) STO films grown with different PEI molecular weights are shown in figure 2, respectively. It is clearly seen that only (*l*00) diffraction peaks

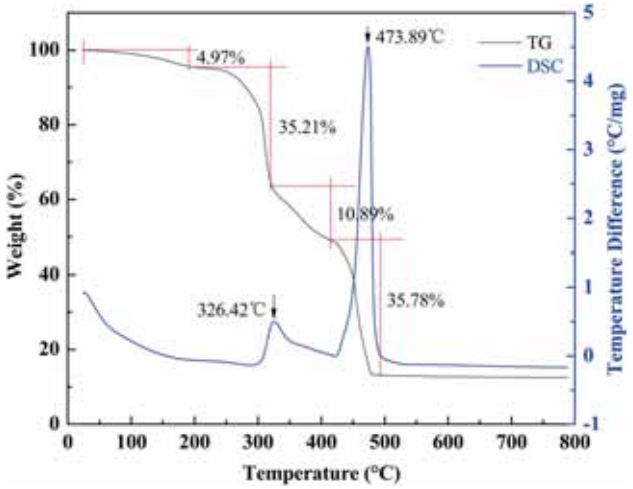

Figure 5. TG/DSC curves of the precursor for preparing LCO films. PEI dose not decompose completely until 500°C.

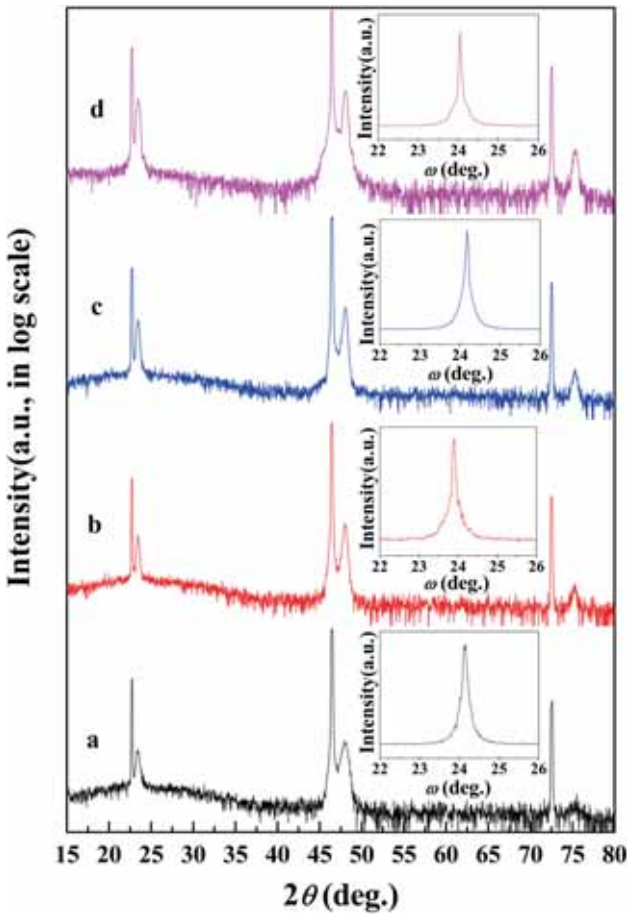

Figure 6. XRD patterns of $\theta/2\theta$ scans for the LCO films calcined at different temperatures: (**a**) 600, (**b**) 700, (**c**) 800 and (**d**) 900°C, respectively. Films prepared at higher temperature have better crystallinity. The insets show the ω-scans (rocking curves) of the (200) peaks for these LCO films.

Table 1. Out-of-plane (c) lattice parameters and FWHM of rocking curves for (200) peaks of LCO films calcined at 600, 700, 800 and 900°C, respectively.

Calcination temperature (°C)	600	700	800	900
c (Å)	3.808	3.799	3.792	3.789
FWHM (°)	0.252	0.237	0.216	0.179

of LCO can be detected, all accompanied by the STO (l00) diffraction peaks. It means that the LCO thin films have a good c-axis orientation [14,25]. Compared with the diffraction peaks of (100) STO and (200) STO located at 22.75° and 46.50°, the (100) and (200) peaks of the LCO all appear at higher 2θ angles, 23.36° and 47.90°, respectively. However, the (l00) LCO peaks of films grown with PEI of smaller molecular weight (M = 600, 1800) are very weak. The results indicate that the PEI with larger molecular weight is favourable to the formation of LCO epitaxial films.

On the basis of XRD result, the chelating characteristics of metal ions by PEI with different molecular weights may have important influence on the growth of LCO epitaxial film, resulting in different crystallinities and epitaxial qualities. To gain a better understanding of the key functional groups in PEI, the IR spectra of PEI with different molecular weights were studied. Figure 3 shows the IR spectra of PEI with different molecular weights (M = 600, 1800, 10 k and 70 k). As is known, the absorption at ~3400 cm^{-1} belongs to the N–H stretching vibration of –NH, while the peak at ~3300 cm^{-1} is assigned to the N–H stretching vibration of $–NH_2$ [26–30]. Obviously, in figure 3, with the increase of PEI molecular weight, the peak intensity of N–H stretching vibration of –NH (peak I) increases and peak width narrows, while the peak intensity of N–H stretching vibration of $–NH_2$ (peak II) gradually decreases and finally disappears (figure 3d). The absorption at ~1655 cm^{-1} (peak III) is the N–H bending vibration of $–NH_2$, which changes from strong to weak with the increase of PEI molecular weight. Furthermore, the N–H bending vibration peak of –NH at ~1570 cm^{-1} (peak IV) appears and increases gradually. It clearly indicates that there are more –NH, but less $–NH_2$ in PEI with larger molecular weight (M = 10 k, 70 k). According to Gao's [21] and Jia's [31] researches, the cations in PEI derive from the protonation of amino groups, while the ability of amino groups to accept protons is related to the size of the electron cloud density at the nitrogen atom. From the electron-induced effect, the number of hydrocarbon groups on –NH is more than that on $–NH_2$, resulting in the electronic cloud density on –NH greater than that on $–NH_2$. That is to say the protonation ability of –NH is stronger. Therefore, the chelating capacity of PEI with larger molecular weight (M = 10 k, 70 k) is better because they have more –NH. This result is consistent with the research of Fischer [32], who found that the contribution of the high chelating ability of PEI was mainly due to the secondary amino groups in the molecule.

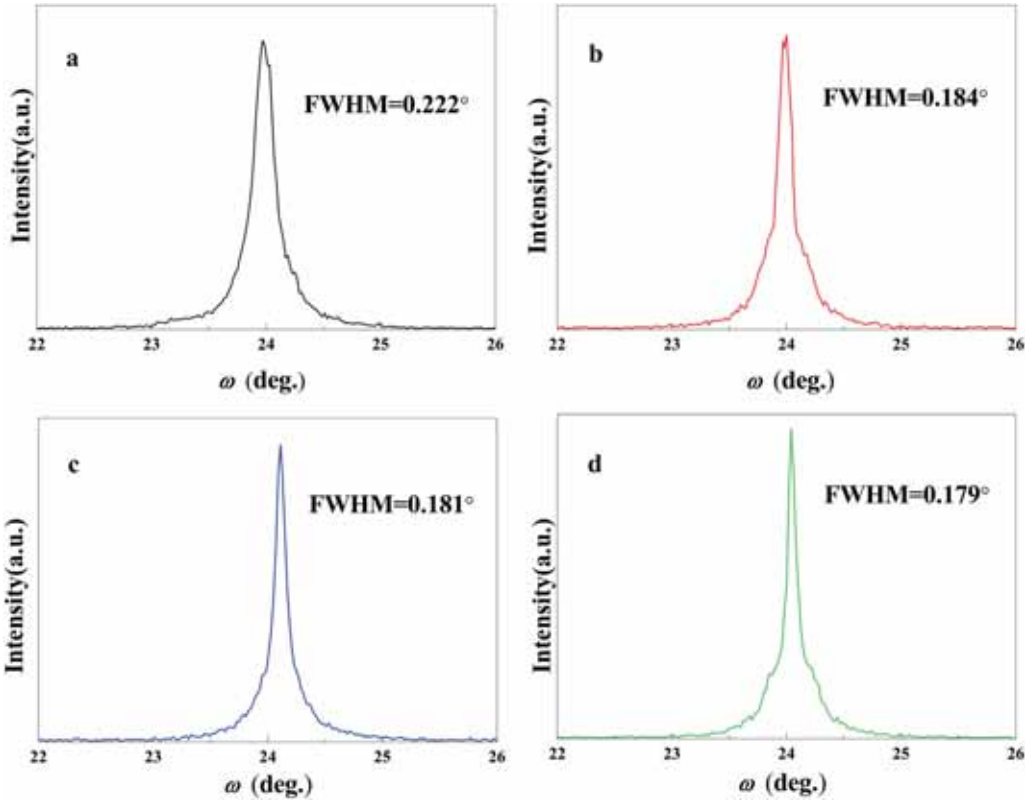

Figure 7. The ω-scans (rocking curves) of the (200) peaks for the LCO films grown at different heating rates: (**a**) 1, (**b**) 4, (**c**) 7 and (**d**) 10°C min^{-1} when PEI begins to release the bound metal ions at around 500°C, respectively. The FWHM values decrease with the increase in heating rate.

Moreover, the bonding characteristics of chelates obtained with PEI of different molecular weights were also investigated through IR spectra (see figure 4). It can be found that the broad and smooth absorption bands between 3300 and 3600 cm^{-1} (peak V) are intermolecular hydrogen bonds or O–H stretching vibration in water molecules. The absorption peaks near 2920 cm^{-1} are the stretching vibration of C–H bond, and its intensity decreases gradually with the increase in the molecular weight of PEI, which even disappears when $M = 70$ k (see figure 4d) comparing with that of the pure PEI in figure 3. This may be related to the formation of hydrogen bonds, which makes the O–H associate, and the associated O–H will cover the C–H stretching vibration. Additionally, the disappearance of N–H bending vibration peaks of $–NH_2$ and –NH (peak III and peak IV in figure 3) indicates that the amino groups were substantially consumed during precursor formation process. And the absorption peaks at ∼1600 cm^{-1} (peak VI) are coordinated –COO stretching vibration of metal–EDTA chelate. The absorption at 1384 cm^{-1} (peak VII) is related to C–H bending vibration. Besides, the stretching vibration peaks of C–O bond at ∼1100 cm^{-1} (peak VIII) are gradually decreased with the increase of PEI molecular weight, which may be associated with the formation of N–M (La or Co)–O bond (∼1030 cm^{-1}). Then the stretching vibration absorption peak of NO_3^- is located at 720 and 830 cm^{-1}. It appears jagged absorption band between 500 and 700 cm^{-1}, which is the stretching vibration of M–O, O–M–O and C–O–M bonds [33,34]. No stretching vibration of noncoordinated –COO is observed in the spectra, it reveals that all the EDTA has reacted to become M–EDTA and formed ligands with PEI. Based on the above discussion, it is known that the number of –NH groups plays a key role on the cation-chelation of PEI. There are relatively more –NH groups existing in PEI with larger molecular weight, which contribute to the improvement of the crystallinity and epitaxial quality.

3.3 *Effect of heat-treatment condition on the crystallinity and epitaxial quality of LCO films*

The thermal decomposition characteristics of the precursor for LCO films were analysed by thermogravimetric and differential scanning calorimetry analysis (TG/DSC) as shown in figure 5. It can be clearly seen that there are four main weight loss regions in the range of room temperature to 800°C. The weight loss between the room temperature and 200°C is mainly due to the volatilization of physically adsorbed water. Among 200−320°C, it shows a significant weight loss, mainly caused by the loss of crystal water, nitrate and EDTA decomposition, and this process is carried out quickly [34]. The weight loss from 320 to 420°C is due to the decomposition of

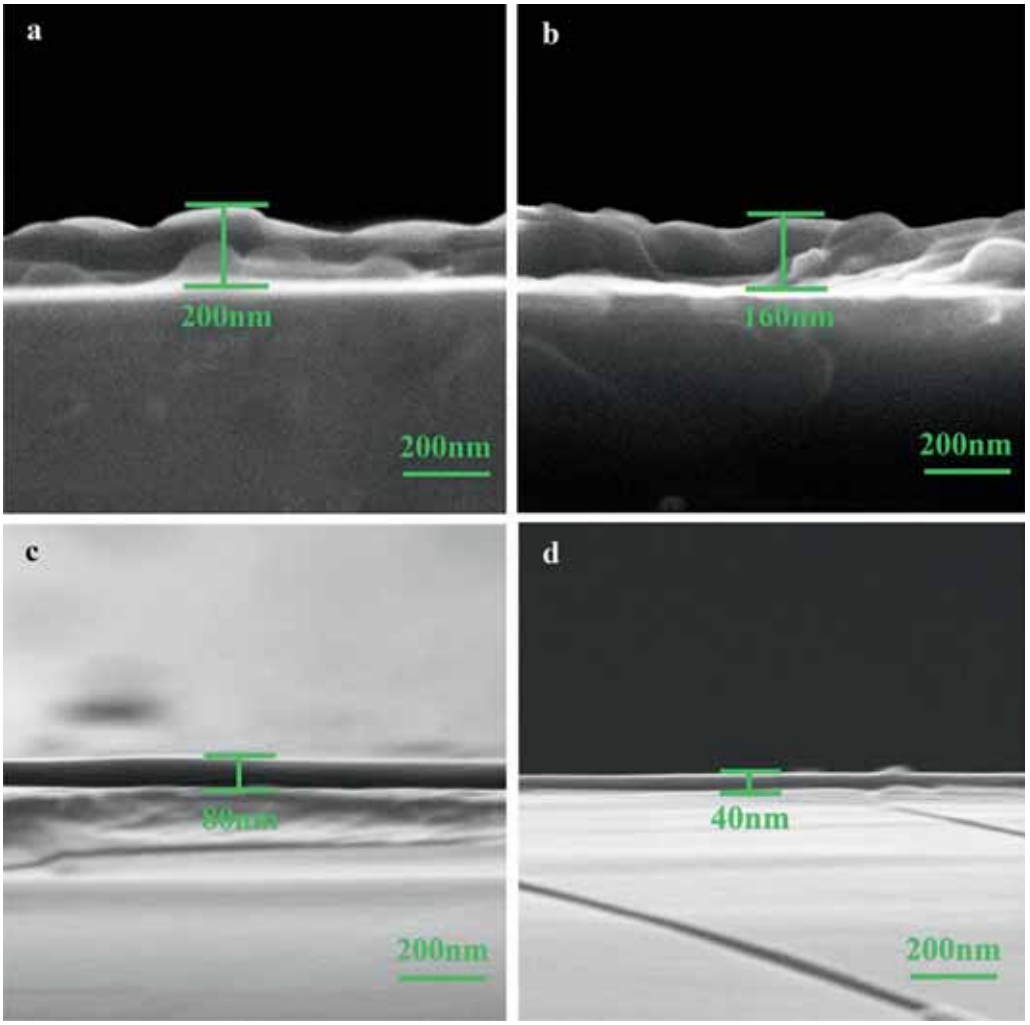

Figure 8. The cross-section of FESEM images of the LCO films prepared by different spin-coating speeds: (**a**) 2000, (**b**) 4000, (**c**) 5500 and (**d**) 7000 rpm, respectively. Higher spin-coating speed corresponds to thinner, smoother and denser films.

the polymer chains. The volatilization of the residue occurrs at 420−500°C, which brings about 35.78% weight loss. Accordingly, two exothermic peaks (326.42 and 473.89°C) appear in the corresponding region of the DSC curve. It means that the temperature at which PEI begins to decompose is about 320°C, but it dose not decompose completely until 500°C. Thus, to prevent the film from pinholes and cracks, even formation of polycrystalline in the process of heat treatment owing to fast heating rate, the temperature should be increased at a relatively slower rate from room temperature to 500°C. The huge exothermic peak at 473.89°C corresponds to the formation of LCO crystals, and the process of LCO crystals gradually become the crystalline from 500 to 600°C, which is consistent with Jain's study [15]. However, based on Kwon's research [7], nucleation can be initiated not only on the surface of the substrate, but also away from the surface of the substrate when the polymer is burnt at 500°C. Therefore, a relatively higher temperature with fast heating rate may be conducive to improve the crystallinity and epitaxial quality of LCO films.

To study the relationship between epitaxial quality of LCO epitaxial films and heat treatment temperature, the (100) STO substrate coated with LCO thin film was calcined at 600, 700, 800 and 900°C in air atmosphere, respectively. The relevant XRD patterns of the prepared samples are shown in figure 6. Similarly, there are only (*l*00) LCO peaks at different calcination temperatures. Moreover, as the temperature increases, (300) diffraction peak of LCO begins to appear and its diffraction peak intensity gradually enhances. It shows the films prepared at higher temperature have better crystallinity. The out-of-plane ω-scans (rocking curves) of the (200) LCO peaks are shown in the insets of figure 6 and the relevant full widths at half-maximum (FWHM) values are presented in table 1. It can be seen that only the rocking curve corresponding to the (200) plane of the LCO film is detected within a wide range of ω angles, and the peak shape is narrow and sharp.

The FWHM values are approximate and tend to decrease with increasing temperature, which also show the films prepared at higher temperature have better crystallinity. What's more, the out-of-plane (c-axis) lattice parameters of LCO film calcined at different temperatures is calculated by Bragg's Law $d_{hkl} = \lambda/2 \sin \theta_{hkl}$, respectively (see table 1) [35,36]. As the temperature increases, c-axis lattice parameters exhibit slight decreasing trend, suggesting that high deposition temperature helps to improve the epitaxial quality of the film.

In addition, heating rate also has a certain influence on the crystallinity of the epitaxial films. When the temperature reaches 500°C, the LCO thin films were heat-treated at different heating rates, i.e., 1, 4, 7 and 10°C min^{-1}, respectively. The out-of-plane ω-scans of the (200) LCO peaks are shown in figure 7. The experimental results show that the FWHM values have a downward trend with the increase in heating rate. This phenomenon indicates that a relatively rapid rate of heating after 500°C can effectively prevent nucleus from growing in other orientations, thereby improving the quality of film crystallization and leading to a good orientation, which is aligned with Kwon's research mentioned above [7].

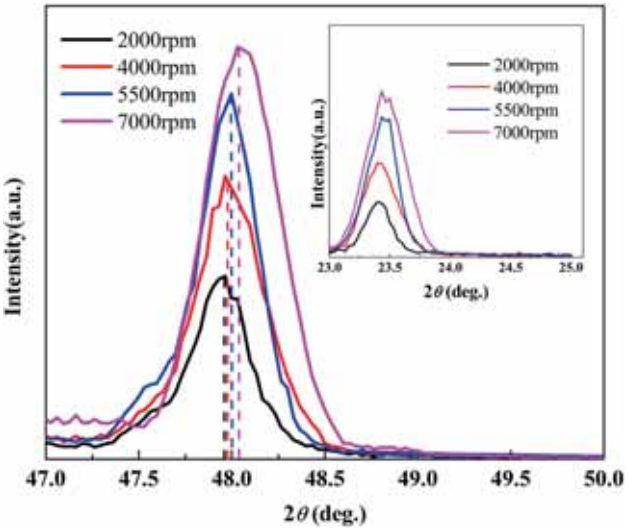

Figure 9. XRD patterns of $\theta/2\theta$ scans for the (200) LCO prepared by different spin-coating speeds. The insets show the diffraction peak of (100) LCO. The out-of-plane (c) lattice parameters decrease with the increase in spin-coating speed.

3.4 *Effect of spin-coating speed on the crystallinity and epitaxial quality of LCO films*

The cross-section of FESEM micrographs of the LCO thin films prepared by different spin-coating speeds (2000, 4000, 5500 and 7000 rpm) is shown in figure 8. It can be found that the thicknesses of the LCO films, obtained at spin coating speed of 2000, 4000, 5500 and 7000 rpm, are around 200, 160, 80 and 40 nm, respectively. Moreover, spin-coating speed also has influence on the surface roughness and compactness of the film. Obviously, higher spin-coating speed is corresponding to thinner, smoother and denser films. Therefore, it is possible to adjust the film thickness and surface roughness by controlling the spin-coating speed, while maintaining the other spin-coating parameters as constant [17].

Additionally, figure 9 shows the XRD spectra of LCO epitaxial films prepared by different spin-coating speeds. As can be seen, with the increase of spin-coating speed, the position of the (200) and (100) plane diffraction peaks of LCO thin films regularly shifted to high angles, which means that the unit cell parameters of the c-axis show a gradually decreasing trend. The reason for this phenomenon is the lattice relaxation in the epitaxial films [5]. With the increase in the thickness of LCO film, the two-dimensional tensile stress on the surface of film from STO substrate is slightly relaxed and gradually becomes smaller, leading to a slight increase in the average c-axis unit cell parameter. What's more, the decomposition of PEI during the thermal treatment of the film may help in the formation of micropores. The number of these micropores also increases with the increase in film thickness, which may lead to lattice relaxation of the epitaxial film. Consequently, during the preparation of thin film materials by spin-coating method, the choice of spin speed will directly affect the thickness of the film, and may even affect the structure and performance of the film.

4. Conclusions

To summarize, LCO epitaxial films were grown on single-crystal (100)-oriented STO substrates by the simple polymer-assisted deposition. The structural and morphological characteristics prove that LCO epitaxial films were grown on (100) STO substrates successfully. It is found that the number of –NH groups plays a key role in the cation-chelation of PEI. There are relatively more –NH groups existing in PEI with larger molecular weight, which contribute to the improvement of the crystallinity and epitaxial quality. Moreover, when PEI begins to release the bound metal ions at around 500°C, higher heat-treatment temperature and a relatively rapid rate of heating can effectively prevent nucleus from growing in other orientations, thereby improving the epitaxial quality of film. Besides, the choice of spin speed will directly affect the thickness and surface roughness of the film, and may even affect the structure and performance of the film.

Acknowledgements

This work was supported by the National Natural Science Foundation of China (grant no. 51502249); the Scientific Research Fund of Education Department of Sichuan Province (grant nos. 16ZA0133 and 15ZB0108); and the Doctoral Foundation of Southwest University of Science and Technology (grant no. 15zx7105).

References

[1] Gawne D T, Bao Y Q, Gao J M, Zubizarreta C, Goikoetxea J and Barriga J 2013 *Surf. Coat. Technol.* **236** 388

[2] Warwick M E A and Binions R 2013 *Surf. Coat. Technol.* **230** 28

[3] Zhu T, Deng Z H, Fang X D, Dong W W, Shao J Z, Tao R H *et al* 2016 *Bull. Mat. Sci.* **39** 883

[4] Posadas A, Berg M, Seo H, Smith D J, Kirk A P, Zhernokletov D *et al* 2011 *Microelectron. Eng.* **88** 1444

[5] Herklotz A, Rata A D, Schultz L and Dörr K 2009 *Phys. Rev. B* **79** 092409

[6] Zhi M Y, Huang W X, Shi Q W, Wang M Z and Wang Q B 2016 *RSC Adv.* **6** 67488

[7] Kwon T, Ohnishi T, Mitsuishi K, Ozawa T C and Takada K 2015 *J. Power Sources* **274** 417

[8] Lv P P, Yang C H, Geng F J, Feng C, Jiang X M and Hu G D 2016 *J. Sol–Gel Sci. Technol.* **78** 559

[9] Arai T, Ohno T, Matsuda T, Sakamoto N, Wakiya N and Suzuki H 2016 *Thin Solid Films* **603** 97

[10] Yilmaz C and Unal U 2015 *RSC Adv.* **5** 16082

[11] Jia Q X, McCleskey T M, Burrell A K, Lin Y, Collis G E, Wang H *et al* 2004 *Nat. Mater.* **3** 529

[12] Liu H F, Shi L, Zhou S M, Zhao J Y, Guo Y Q, Wang C L *et al* 2013 *Surf. Coat. Technol.* **226** 108

[13] Yue F, Huang W X, Shi Q W, Li D X, Hu Y Y, Xiao Y *et al* 2014 *J. Sol–Gel Sci. Technol.* **72** 565

[14] Yao D, Shi L, Zhou S M, Liu H F, Wang Y, Zhao J Y *et al* 2016 *J. Phys. D: Appl. Phys.* **49** 125301

[15] Jain M, Lin Y, Shukla P, Li Y, Wang H, Hundley M F *et al* 2007 *Thin Solid Films* **515** 6411

[16] Xie C Z, Shi L, Zhou S M, Zhao J Y, Liu H F, Li Y *et al* 2015 *Surf. Coat. Technol.* **277** 222

[17] Liu H F, Shi L, Guo Y Q, Zhou S M, Zhao J Y, Wang C L *et al* 2014 *J. Alloys Compd.* **594** 158

[18] Liu Y, Hu J, Li Y, Wei H P, Li X S, Zhang X H *et al* 2015 *Talanta* **134** 16

[19] Mishra A, Kumar J and Melo J S 2017 *Biosens. Bioelectron.* **87** 332

[20] Rivadulla F, Bi Z X, Bauer E, Rivas-Murias B, Vila-Fungueirino J M and Jia Q X 2013 *Chem. Mater.* **25** 55

[21] Gao B J, An F Q and Liu K K 2006 *Appl. Surf. Sci.* **253** 1946

[22] Molinari R, Poerio T and Argurio P 2008 *Chemosphere* **70** 341

[23] Bessbousse H, Rhlalou T, Verchère J F and Lebrun L 2008 *J. Membr. Sci.* **307** 249

[24] Kobayashi S, Shirasaka H, Suh K D and Uyama H 1990 *Polym. J.* **22** 442

[25] Zhang L, Li P, Huang K, Tang Z, Liu G H and Li Y B 2011 *Mater. Lett.* **65** 1696

[26] Liu H F, Guo Y Q, Xie R S and Ma G H 2016 *Nano* **11** 1650030

[27] Wen Y T, Pan S R, Luo X, Zhang W, Shen T and Feng M 2010 *J. Biomater. Sci.: Polym. Ed.* **21** 1103

[28] An F Q and Gao B J 2007 *J. Hazard. Mater.* **145** 495

[29] Jia Y R, Zhang Y, Liu G J, Zhuang G Q, Fan Q G and Shao J Z 2015 *J. Coat. Technol. Res.* **12** 1031

[30] Gao B J, Jiang P F and Lei H B 2006 *Mater. Lett.* **60** 3398

[31] Jia J, Luan S J and Wu A H 2014 *Polym. Bull.* **11** 34

[32] Fischer D, Harpe A V, Kunath K, Petersen H, Li Y and Kissel T 2002 *Bioconjugate Chem.* **13** 1124

[33] Li S L, Zhu X D, Sun L C and Ao Q 2013 *Chinese Rare Earths* **3** 010

[34] Zhu C F, Xue J H, Wang L and Wang X J 2010 *Chin. J. Inorg. Chem.* **26** 1165

[35] Rata A D, Herklotz A, Schultz L and Dörr K 2010 *Eur. Phys. J. B* **76** 215

[36] Fuchs D, Arac E, Pinta C, Schuppler S, Schneider R and Löhneysen H V 2008 *Phys. Rev. B* **77** 014434